

Data Reconciliation and Control in Styrene-Butadiene Emulsion Polymerizations

Paula Naomi Souza,¹ Matheus Soares,¹ Marcelo M. Amaral,² Enrique Luis Lima,¹ José Carlos Pinto^{*1}

Summary: A nonlinear model-based predictive control (NLMPC) method was developed using a First Principles model of an emulsion copolymerization of carboxylated styrene butadiene rubber (XSBR). Copolymer composition, conversion and average molecular weights of the copolymer were chosen as the controlled variables due to their influence on the final product properties and quality. These properties, however, are rarely measured in-line due to the operational difficulties associated with their measurement. For this reason a soft-sensor using reaction calorimetry techniques was developed and used to infer reaction conditions, rates, species concentrations and polymer properties in a industrial scale emulsion polymerization reactor.

Keywords: calorimetry; copolymerization; emulsion polymerization; predictive control; soft sensor

Introduction

Latexes are commonly produced via emulsion polymerization and their applications cover a wide variety of products, such as paints, adhesives, coatings and varnishes.^[1,2] Emulsion polymerization is one of the most important processes employed for production of synthetic polymers,^[1,2] presenting advantages that include the high molecular weights that can be obtained, the relatively low viscosity of the reaction medium and the easier control of the reaction temperature. Problems associated with sample preparation and general non-observability of the reaction media (polymer particles) make in-line monitoring virtually impossible and constitute some disadvantages of the emulsion polymerization technique.^[3–5]

The end-use properties of a polymer resin can be linked to the molecular properties of the material such as the

molecular weight distribution and the copolymer composition and it is well known that the final polymer properties depend on the whole kinetic and process history. A thorough understanding of the complex nature of emulsion processes can be advantageous in that flexible control schemes can be developed to allow for safer operation under tighter restrictions. Particularly, there is a growing demand for homogenous and higher quality products as a result of growing market competitiveness.^[5]

The lack of appropriate sensors for online monitoring of polymer properties poses a big problem for process control.^[6] The extreme exothermicity of polymerization reactions can be exploited through calorimetry to calculate reaction rates and infer polymer properties; however, there are quite a few reports of reaction calorimetry techniques that have managed to successfully monitor polymer properties in real industrial environments.^[2,7–9] Calorimetry techniques can be used for development of soft-sensors, linking easy to measure variables, such as pressure and temperature measures, to harder (or even impossible) to measure variables through

¹ Programa de Engenharia Química / COPPE, Universidade Federal do Rio de Janeiro, Cidade Universitária, CP: 68502, Rio de Janeiro 21941-972 RJ, Brazil E-mail: pinto@peq.coppe.ufrj.br

² Accenture, Av. República do Chile 500, Centro, Rio de Janeiro 20031-170 RJ, Brazil

the use of a detailed mathematical model. The first-principles model developed for the soft-sensor can then be used in a nonlinear model-based control for calculation of optimal dynamic trajectories and production of polymer resins with particular desired properties in minimum time.

Process Description

In this work, the seeded semibatch emulsion copolymerization of styrene and butadiene was studied. In the process studied, polymer particles are loaded first into the reactor while initiator, chain transfer agent and monomers are fed during the course of the reaction following a strict pre-established policy. Polymer seeds consist of homogeneous polystyrene particles produced prior to the copolymerization. The polymerization is carried out in a semi continuous stirred batch reactor equipped with temperature and pressure sensors, in the presence of small amounts of carboxylic acid monomers. Temperature and pressure readings are available every five seconds, although larger sampling times (5 minutes) are used for monitoring and control purposes, due to the slow reaction dynamics.

Modeling of an Emulsion Copolymerization

The main components of the emulsion polymerization system are the suspending medium (water), the monomers, the polymer material, the water-soluble initiator and the surfactant, which form five different phases: the aqueous medium, the monomer droplets, the micelles, the polymer particles and the gas phase.^[10] It is assumed here that the reaction follows the classical free-radical mechanism^[11] and that particle nucleation follows the classical micellar nucleation mechanism^[11,12] in the presence of seed particles. In order to describe the evolution of the molecular weight averages and compositions of the produced polymer

material, the well-known method of moments is applied^[13,14] As chain transfer to polymer chains cannot be neglected, a moment closure equation is also needed.^[14,15] As a consequence, the mathematical model comprises a system of 14 coupled differential equations that account for the mass balances of the individual reaction components, the moment equations of dead polymer chains and the energy balances. Additional algebraic equations are used to represent the thermodynamic equilibrium constraints, the chemical reaction kinetics and the moments of the living polymer chains. It is important to emphasize that the average number of radicals per particle (n) is calculated with the help of a dynamic mass balance equation, as described in the literature;^[16] therefore, n is allowed to vary during the reaction course. This is particularly important in the beginning of the batch, as the initial initiator concentration was always equal to zero during the actual industrial runs in order to prevent reaction runaway. (Model equations are not presented here for lack of space, but are presented elsewhere.^[12,17,18])

Soft-Sensor and Controller Implementation

The model described previously was used to develop a soft-sensor and model-based nonlinear predictive controller. Both the soft-sensor and controller were implemented in FORTRAN, using optimization and integration routines available within the IMSL library. In order to describe the process operation, natural process variability was incorporated into the model through in-line and real time estimation of the overall heat transfer coefficient (UA) and of a correction factor (α), used to multiply the overall concentration of living radicals ($n \cdot N_T$) and fit the calculated reaction rate profiles. Parameter estimation was based on available reactor pressure, reactor temperature and jacket temperature profiles, given the initial recipe and the

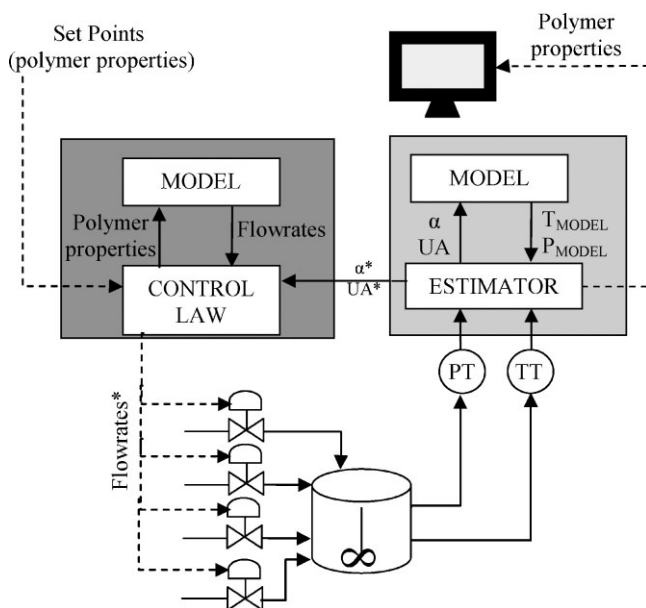


Figure 1.
Soft-sensor and controller.

feed rate policies and using standard least-squares procedures. The soft-sensor outputs were the reactor compositions, the molecular weight averages and compositions of the produced polymer and the parameter estimates, which cannot be measured independently in real time.

After estimation of model parameters and state variables, the calculated data were then fed into the control algorithm to calculate optimum monomer, initiator and modifier feed rate profiles with the aim of obtaining a desired polymer product in minimum time, through minimization of standard weighted square functions.^[12,19] The block diagram presented in Figure 1 represents the estimation and control scheme implemented at plant site. The proposed estimation scheme was implemented at plant site and the performances of the estimator and of the model were tested and validated for different batches, as shown in Figures 2 and 3.

One can observe that there is very good agreement between the calculated temperature and pressure values and the real values. Simulation time was approximately

equal to 30 seconds for the whole polymerization process, making the program adequate for online applications. It can also be observed in Figures 2 and 3 that the fitting parameter α remains close to 1 during a great portion of the reaction, implying that model assumptions seem to be appropriate. Figures 2 and 3 also show that different dynamic trajectories can be expected in different batches, as also observed at plant site. This can definitely justify the implementation of similar data reconciliation schemes at plant, in order to adjust the operation conditions for the actual dynamic trajectories experienced by the process. Particularly, fluctuation of heat transfer coefficients is very high in Batch 2, due to undesired fluctuation of the cooling jacket operation conditions. One can also observe that heat transfer coefficients decrease very significantly in the end of the batch, due to the significant increase of the emulsion viscosity and buildup of a thin polymer film on the internal reactor surfaces. The posterior increase of the heat transfer coefficients is due to reaction halting procedures.

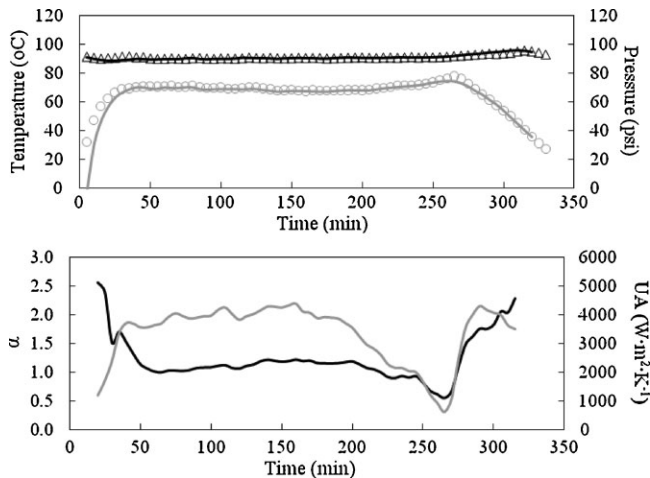


Figure 2.

Comparison between process data and model outputs in Batch 1 (Δ real T; — calculated T; \circ real P; — calculated P). Estimated parameter values. (— α ; — UA).

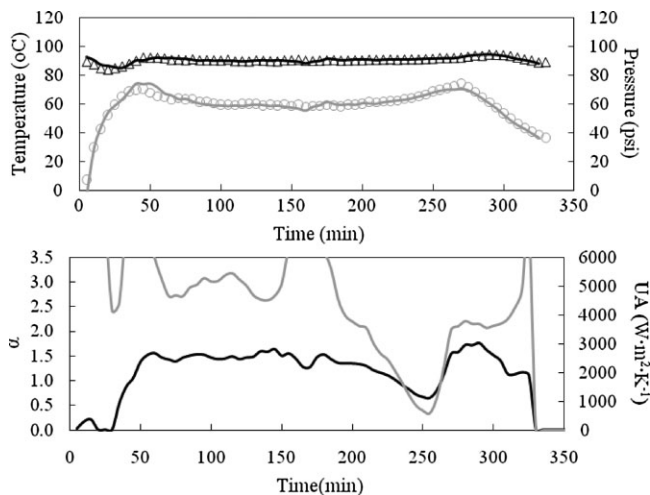


Figure 3.

Comparison between process data and model outputs in Batch 2 (Δ real T; — calculated T; \circ real P; — calculated P). Estimated parameter values. (— α ; — UA).

The aim of the controller is to produce a homogeneous polymer of specified average molecular weight and copolymer composi-

tion in minimum time, according to the minimization of the following objective function:

$$J = \sum_{k=1}^N \left\{ \lambda_{in} \left[\frac{(\bar{i}_{in,Mod})_k - \bar{i}_{in,SP}}{\bar{i}_{in,SP}} \right]^2 + \lambda_{in} \left[\frac{(\bar{i}_{w,Mod})_k - \bar{i}_{w,SP}}{\bar{i}_{w,SP}} \right]^2 + \lambda_{Xcomp} \left[\frac{(X_{comp,Mod})_k - X_{comp,SP}}{X_{comp,SP}} \right]^2 \right\} + \lambda_{in} \left[\frac{(\bar{i}_{in,Mod})_N - \bar{i}_{in,SP}}{\bar{i}_{in,SP}} \right]^2 + \lambda_{in} \left[\frac{(\bar{i}_{w,Mod})_N - \bar{i}_{w,SP}}{\bar{i}_{w,SP}} \right]^2 + \lambda_{Xcomp} \left[\frac{(X_{comp,Mod})_N - X_{comp,SP}}{X_{comp,SP}} \right]^2 + \lambda_t t_f^2 \quad (1)$$

where λ 's are specified weighting values, \bar{i}_n is the number average molecular weight, \bar{i}_w is the weight average molecular weight, X_{comp} is the copolymer composition, t_f is the batch time and k represents the sampling times, where $k=0$ represents the current time and N represents the controller horizon (in the present paper, the end of the batch).

It is important to note that SBR latexes can yield gel polymer because of the propagation to pendant double bonds of the butadiene monomer and of chain transfer to polymer. As a consequence, the end use properties of SBR latexes can be determined in a large extent by the gel content, in addition to the composition of the copolymer and the average molecular weights of the soluble part. Therefore the prediction and control of the gel content can be of paramount importance in this process.^[20,21] Despite that, one must also observe that the final gel content of the latex depends heavily on the copolymer composition and is certainly related to the average molecular weights of the polymer material, as the rates of chain transfer to polymer increase with the butadiene content and larger polymer chains are more likely to present branches than smaller ones. Therefore, successful modeling and control of the copolymer composition and molecular weight averages can allow for

subsequent modeling and control of the gel content of the final SBR latex.

In the particular case analyzed here, the weight average molecular weight of the SBR product is below 5.0×10^6 Da, as large amounts of chain transfer agents are fed into the reactor vessel. The produced latexes are used for covering of paper sheets and fibers. As a consequence, the gel yield of the final polymer material is low, allowing for simplification of the control problem, as computed molecular weight averages are finite and the moments technique can be used for computation of the molecular weight averages in the process model.

Based on Equation (1), optimum feed rate profiles for styrene, butadiene, initiator and chain transfer agent can then be computed and compared to available plant data. For instance, Figures 4 and 5 show optimum feed rate profiles when constraints are not imposed on the process productivity. Calculated optimum feed rate profiles are compared to real constant feed rate profiles, as practiced at the industrial site. It can be observed that specified copolymer composition, and average molecular weights can be controlled very tightly (although not measured) when monomer feeding is concentrated in the beginning and in the end of the batch and reaction pressures and temperatures are kept at

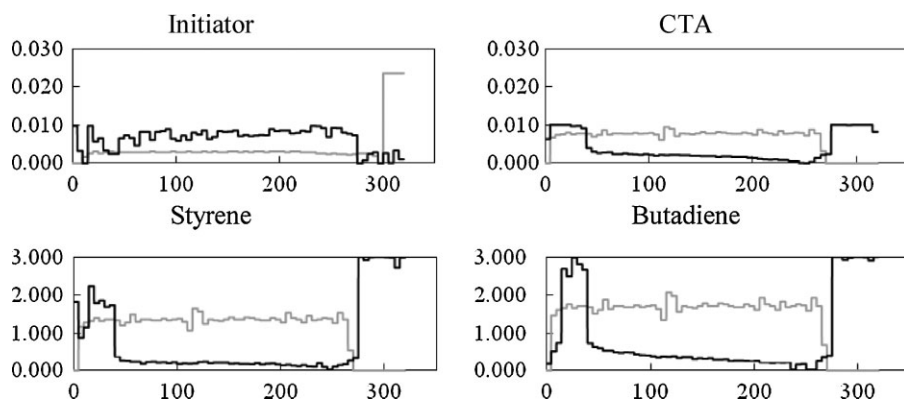


Figure 4.

Calculated initiator, CTA, styrene and butadiene feed rate profiles and comparison with real industrial process data (— controlled; — industrial), when constraints are not imposed on the operation conditions.

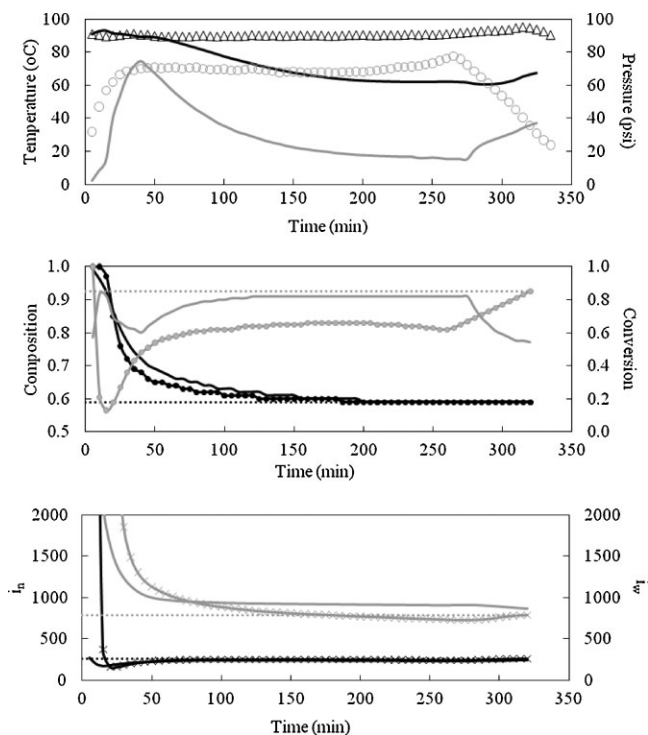


Figure 5.

Pressure and temperature profiles (Δ industrial T; — controlled T; ○ industrial P; — controlled P). Composition and conversion (● industrial composition; — industrial composition; composition setpoint; ◆ industrial conversion; — controlled conversion; ... conversion setpoint). Average molar weights (× industrial i_n ; — controlled i_n ; ... i_n setpoint; × industrial i_w ; — controlled i_w ; ... i_w setpoint), when constraints are not imposed on the operation conditions.

sufficiently low values. However, this operation policy is not economically feasible and cannot be implemented at plant site at all, meaning that operation constraints are of fundamental importance for development of real operation procedures.^[22] It is important to acknowledge this point explicitly, as the existence of operation constraints can lead to poorer control of the polymer properties.

Figures 6 and 7 show results obtained when the reaction batch is expected to be performed in minimum time. Calculated optimum feed rate profiles are compared to real constant feed rate profiles, as practiced at the industrial site. As one can see, in this case reactor temperatures and pressures are kept at much higher values than observed previously and feeding rates are kept at the

maximum allowed operation values in order to keep the copolymer composition and average molecular weights at the desired values. Although obtained results can be regarded as obvious, once again calculated operation policies are not feasible, given the very low monomer conversion values observed during the reaction (which can lead to reaction runaway^[18]), including the very low solids content obtained at the end of the batch. As observed in the previous case, optimum plant operation depends heavily on the proper design of operation constraints that must be satisfied during the batch, which cannot be performed without careful safety and economical reasoning.

Figures 8 and 9 show results obtained when hard constraints were imposed on the

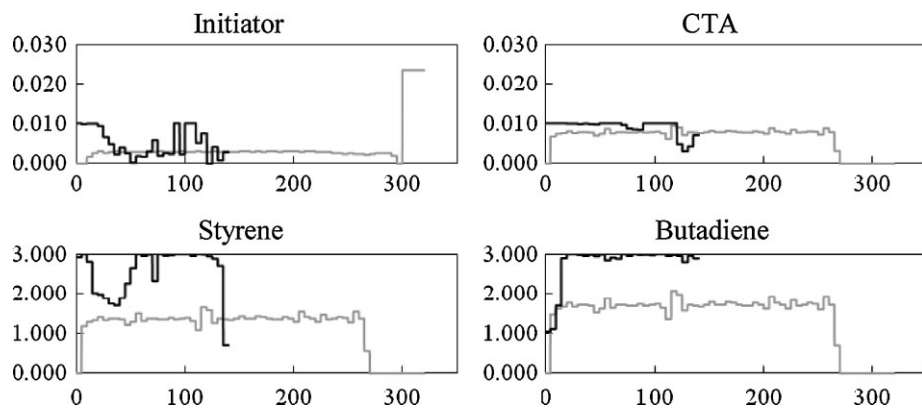


Figure 6.

Calculated initiator, CTA, Styrene and Butadiene feed profiles and comparison with real industrial process data (— controlled; — industrial), when the batch must be performed in minimum time.

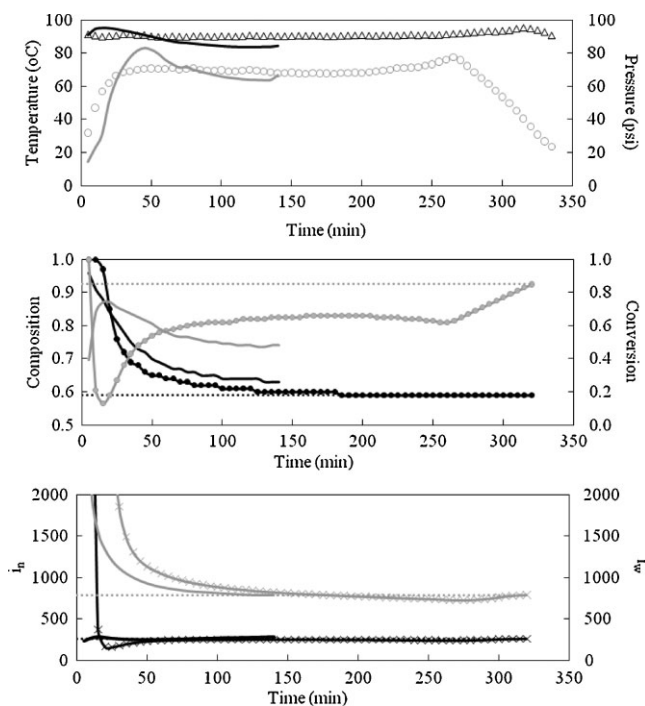


Figure 7.

Pressure and temperature profiles (Δ industrial T; — controlled T; \circ industrial P; — controlled P). Composition and conversion (\blacklozenge industrial composition; — industrial composition; ... composition setpoint; \blacklozenge industrial conversion; \circ controlled conversion; ... conversion setpoint). Average molar weights (\blacklozenge industrial i_n ; — controlled i_n ; ... i_n setpoint; \blacklozenge industrial i_w ; — controlled i_w ; ... i_w setpoint), when the batch must be performed in minimum time.

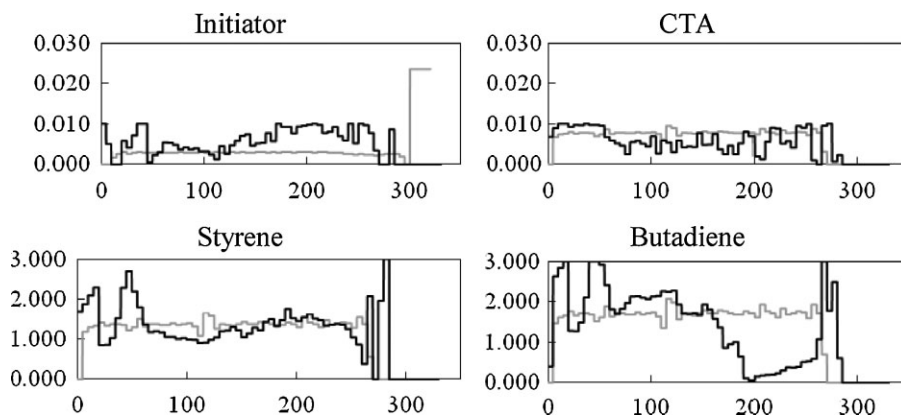


Figure 8.

Calculated initiator, CTA, Styrene and Butadiene feed profiles and comparison with real industrial process data (— controlled; — industrial), when hard constraints were imposed on the trajectory of monomer composition.

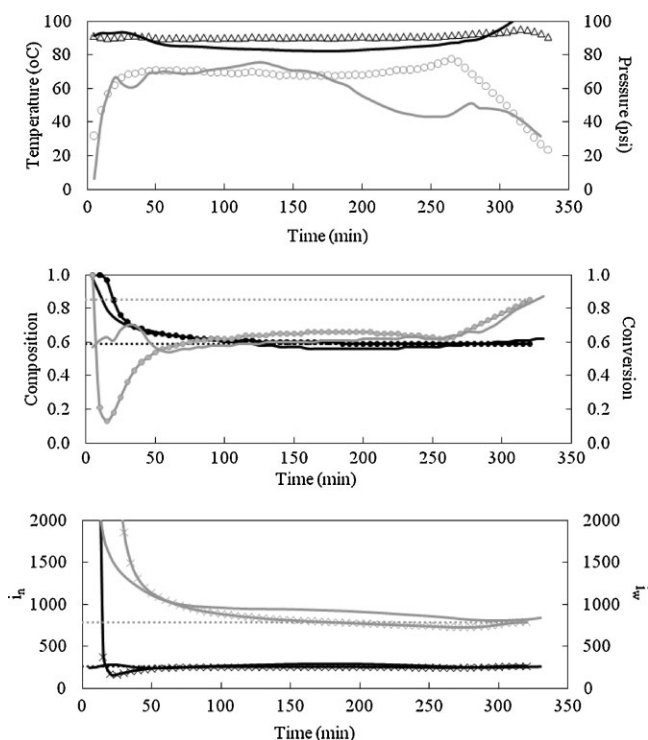


Figure 9.

Pressure and temperature profiles (Δ industrial T; — controlled T; \circ industrial P; — controlled P). Composition and conversion (\blacktriangle industrial composition; — industrial composition; composition setpoint; \blacklozenge industrial conversion; \circ controlled conversion; conversion setpoint). Average molar weights (\blacktimes industrial i_n ; — controlled i_n ; i_n setpoint; \blacktimes industrial i_w ; — controlled i_w ; i_w setpoint), when hard constraints were imposed on the trajectory of monomer composition.

trajectory of monomer conversion. Calculated optimum feed rate profiles are compared to real constant feed rate profiles, as practiced at the industrial site. In this case, the minimum allowed conversion values was equal to 0.65, in order to avoid the formation of the monomer phase, while the final monomer conversion was not allowed to be lower than 0.90 for economical reasons (consumption of unreacted monomer and final monomer stripping were carried out in a second reactor tank during latex preparation). According to Figures 8 and 9, optimum operation conditions followed the plant operation conditions very closely, although important changes could be noticed in the beginning and in the end of the batch. For instance, optimum initial feed rates were higher than practiced at plant site, for faster filling of the reactor. As a consequence, feed rates were smaller at the end of the batch, given the finite capacity of the reactor vessel. It is also interesting to observe that the higher rates of initiator feeding in the beginning of the batch led to higher initial monomer conversions, avoiding the dangerous accumulation of monomer inside the reactor during the initial hour of reaction. Figure 9 shows that the proposed operation procedure also led to improved control of the reactor temperature during the last part of the batch, as the higher reaction temperatures observed at plant site during this period were due to the finite heat transfer capacity of the reaction equipment.

It is important to point out that the trajectories obtained for all the controlled properties were consistently close to their setpoints even when hard constraints were imposed on the monomer conversion values, as shown in Figure 9. Despite that, one can definitely observe that consistent small deviations to higher molecular weight averages were obtained as a consequence of the higher monomer concentrations, given the relatively large rates of chain transfer to polymer. This indicates once more that the design of process constraints must be performed with care, as the existence of process operation constraints leads to

poorer control of the polymer properties. In the particular case analyzed here, though, it can be shown that manipulation of the solids content can compensate for small deviations of the final molecular weight averages.

Conclusion

The soft-sensor developed in this work allows the monitoring of polymer properties that are otherwise practically immeasurable. The outputs provided by the soft-sensor (unmeasured state variables and estimates for parameters α and UA) can be used to update the model implemented in the controller and to modify the optimum operation trajectory practiced at plant site. As shown through a real industrial example, the proposed control procedure can be indeed implemented in line and in real time for control of the final polymer properties and for maintenance of safe and feasible economic operation conditions. Both soft-sensor and controller are computationally efficient and allow for online applications, using standard numerical procedures available in the literature.

The soft-sensor provides estimates of the reaction conditions such as polymerization rates, amount of unreacted monomer in the reactor and heat transfer rates. Particularly, the proposed controller was used to correct the initial undesired drop in monomer conversion that occurred in the industrial process due to the low feed rates of initiator practiced in the beginning of the batch.

- [1] B. Benyahia, M. A. Latifi, C. Fonteix, F. Pla, S. Nacef, *Chem. Eng. Sci.* **2010**, 65, 850.
- [2] J. Zeaiter, V. G. Gomes, J. A. Romagnoli, G. W. Barton, *Chem. Eng. J.* **2002**, 89, 37.
- [3] C. Sayer, G. Arzamendi, J. M. Asua, E. L. Lima, J. C. Pinto, *Comput. Chem. Eng.* **2001**, 25, 839.
- [4] J. R. Richards, J. P. Congalidis, *Comput. Chem. Eng.* **2006**, 30, 1447.
- [5] B. Alhamad, J. A. Romagnoli, V. G. Gomes, *Chem. Eng. Sci.* **2005**, 60, 6596.
- [6] T. Kreft, W. F. Reed, *Eur. Polym. J.* **2009**, 45, 2288.

- [7] L. M. Gugliotta, M. Arotcarena, J. R. Leiza, J. M. Asua, *Polymer* **1995**, 36, 2019.
- [8] I. S. De Buruaga, M. Arotcarena, P. D. Armitage, L. M. Gugliotta, J. R. Leiza, J. M. Asua, *Chem. Eng. Sci.*, 51, 2781.
- [9] M. Vicente, J. R. Leiza, J. M. Asua, *Chem. Eng. Sci.* **2003**, 58, 215.
- [10] W. D. Harkins, *J. Am. Chem. Soc.* **1947**, 69, 1428.
- [11] G. Odian, “*Principles of Polymerization*”, John Wiley & Sons, New Jersey 2004.
- [12] M. Nomura, H. Tobita, K. Suzuki, *Polymer Particles* **2005**, 175, 1.
- [13] V. Prasad, M. Schley, L. P. Russo, W. Bequette, *J. Process Control* **2002**, 12, 353.
- [14] R. L. Laurence, R. Galvan, M. V. Tirrell, in: “*Polymer Reactor Engineering*”, 1st ed. C. McGreavy, Ed., Blackie Academic & Professional, New York 1994.
- [15] H. M. Hulburt, S. Katz, *Chem. Eng. Sci.* **1964**, 19, 555.
- [16] S. C. Thickett, R. G. Gilbert, *Polymer* **2007**, 24, 6965.
- [17] M. Soares, F. Machado, A. Guimãães, M. Amaral, J. C. Pinto, 9th *Brazilian Congress On Polymers*, **2007**, 1, 1.
- [18] W. V. Smith, R. H. Ewart, *J. Chem. Phys.* **1948**, 16, 592.
- [19] M. Vicente, C. Sayer, J. R. Leiza, G. Arzamendi, E. L. Lima, J. C. Pinto, J. M. Asua, *Chem. Eng. J.* **2002**, 85, 339.
- [20] D. Charmot, J. Guillot, *Polymer* **1992**, 33, 352.
- [21] D. Charmot, J. F. D’Allest, F. Dobler, *Polymer* **1996**, 37, 5237.
- [22] A. R. Secchi, E. L. Lima, J. C. Pinto, *Polym. Eng. Sci.* **1990**, 19, 1209.